High Diversity Gain MIMO-Antenna for UWB Application with WLAN Notch Band Characteristic Including Human Interface Devices

Gaurav Saxena[1,2] · Priyanka Jain[1] · Yogendra Kumar Awasthi[3]

Abstract

In this paper, a UWB–MIMO antenna with the WLAN band-notch (5.1–5.85 GHz) characteristic is offered. This antenna consists of two radiated patch feeding with a tapered line and fabricated on abundantly available FR-4 substrate having the size of $36 \times 22 \times 1.6$ mm^3. A notched-band response is achieved by introducing an open-ended stub on the ground plane. Results illustrate that the designed antenna has an impedance bandwidth from 3.1 to 11.2 GHz as well as good isolation i.e. $S_{21} \leq -30$ dB. Radiation efficiency is greater than 0.75 except the notched band is < 0.5. Diversity performance is also set the new paradigm in terms of ECC (≤ 0.008), TARC (≤ -25 dB), CCL (≤ 0.3 bits/s/Hz), Mean effective gain ratio (MEGi) $\cong 1$ and directive gain (≥ 9.95 dB) except the notched band. Proposed antenna characteristics are also found suitable for a human interface device, low-cost, and easily fabricated. Simulated results of the proposed antenna are tested and verified by the experimental results.

✉ Priyanka Jain
  priyankajain@dtu.ac.in

  Gaurav Saxena
  gaurav.saxena@galgotiacollege.edu

  Yogendra Kumar Awasthi
  yogendra@mru.edu.in

1   Department of Electronics and Communication Engineering, Delhi Technological University, Delhi 110042, India

2   Galgotia College of Engineering and Technology, Greater Noida 201306, India

3   Antenna Fabrication and Measurement Laboratory, Electronics and Communication Engineering, Manav Rachna International Institute of Research and Studies, Faridabad 121004, India

1 Introduction

MIMO antenna is extensively utilized in contemporary wireless RF communication system to improve the diversity problem in a single input single output-SISO antenna. The UWB system operates in a wide range of frequency among small spectral power. The signal to noise ratio is also less at the receiver end. That's why; band-notch is the only opportunity to mitigate the interference from UWB applications through wireless protocols like WiMAX, LTE, and WLAN. The electromagnetic bandgap is used to improve the isolation of the MIMO antenna and co-design approach provides better diversity results [1, 2]. Isolation of MIMO is improved by introducing carbon black film, which can be absorbing the intrusion among antenna elements [3]. Moreover, high isolation is attained by T-shaped slot and stub on the ground plane and dual-polarization (Linear to circular) is achieved by using two perpendicular feeding lines at the patch [4, 5]. In addition, to achieve good isolation performance, T-shaped protuberant ground and Y-shaped quadrate patch are suggested for UWB applications [6]. An extruded T-shaped decoupling structure is introduced in UWB–MIMO antenna to achieve a good diversity performance [7] and orthogonal monopole radiators are also used to attain high isolation without introducing decoupling structure in the ground [8]. Furthermore, by using a T-shaped slot and two-line slots on the ground, high isolation and impedance bandwidth have been achieved [3]. Moreover, inverted L-shaped slits are introduced to produce good diversity performance [9].

By using Monopole antennas, it is achieved UWB operation from 3.1 to 10.6 GHz. In addition, T-shaped slot and stub in the ground are used to minimize the mutual coupling by − 15 dB and two ground-strips are produced an excellent band-notch characteristic for WLAN (5.15–5.85 GHz) to suppress interference [10]. A tapered feed microstrip line with two identical triangular shaped patch radiators and two triangles with J-shaped slit ground are built to get the WLAN notch-band characteristic from 5.10 to 5.85 GHz and INSAT and extended C-band from 6.7 to 7.1 GHz [11]. Henceforth, folded printed monopole antenna is designed to enhance the bandwidth, which is joined with an inverted-L parasitic element and introduced an open-stub to eliminate the WLAN (5.15–5.85 GHz) band [12, 13]. A rectangle shaped stub and split ring resonator (SRR) are providing to attain good isolation and rejection of band simultaneously. Results have shown improved matching of impedance with the required radiation pattern and constant gain also achieved in the operating bandwidth [14]. Moreover, a compact rectangular dielectric resonator (DRA) MIMO antenna with microstrip feed is designed to achieve good bandwidth and inserted two stubs in the ground to get high isolation between antennas [15]. The wireless communication system has various generations (1G–5G), which is supported by SISO to MIMO systems and large bandwidth of the system is one of the foremost factors for high transmission data rate, to enhance the services like triple play i.e. data, audio, and video. Hence, at user end the capacity directly influence the communication system quality. Although MIMO system provides these features in a challenging world to provide high data rate, low channel capacity loss and high signal to noise ratio (SNR) [16] and orthogonal radiating staircase shaped patches with modified co-planer waveguide feed MIMO antenna is designed with 5.5 GHz band-notched characteristics [17]. To provide high isolation and UWB bandwidth with notched band applications, MIMO antennas are presented [18–20]. Henceforth, two antennas placed orthogonally to each other and decoupling structure designed in the ground plane to accomplish better isolation between two radiator elements. To improve isolation in MIMO antenna system, two defective complementary open-loop resonators also used to get required results between antennas [21, 22].

In this paper, two-element tapered fed high diversity gain, WLAN notched UWB–MIMO antenna is proposed and it has fabricated on FR-4 substrate with a compact size of $36 \times 22 \times 1.6$ mm^3. A band-notch characteristic is obtained through two open-ended stubs on the ground. Furthermore, the diversity characteristic of "mean effective gain" MEGi/MEGj ratio and channel capacity loss (CCL) has also studied. Section 2 presents the proposed antenna design procedure. Section 3 elucidates the proposed antenna results and discussion and Section 4 depicts the diversity performance of the proposed antenna. The achieved results of measurement and simulation are in better concurrence.

2 MIMO Antenna Design Procedure

Numerous wideband applications such as microwave medical imaging, ground penetrating radar (GPR) and RFID tag for inventory control and asset management require a compact and inexpensive UWB–MIMO wireless transceivers. UWB–MIMO base station receiver architecture with different blocks is shown in Fig. 1.

Impulse data is transmitted using UWB–MIMO antenna and after that UWB–MIMO receiver antenna receives the data in a different path and produces the base-band signal, where the information is first encoded, digitally modulated, and then converted into pulse using pulse generator. This UWB–MIMO antenna has shown in Fig. 2a and b with WLAN notch is fabricated on FR-4 substrate of height (h) 1.6 mm with relative permittivity (ε_r) of 4.4, loss tangent (tanδ) of 0.02 by the dimension of 36 mm×22 mm. The antenna is designed by a circular with triangular notched patches and to enhance the isolation between two radiated patches, a T–I shaped slot in the ground is groomed, which improves the isolation better than -30 dB in wished-for UWB bandwidth. The resonant frequency of circular patch for TM$_{11}$ mode is 7.15 GHz which is used to calculate the patch radius to achieve desired bandwidth (3.1–11.2 GHz).

UWB bandwidth in MIMO antenna including notch band characteristic is achieved by using a tapered feed line together with the partial tailored ground plane. The fundamental resonance frequency of the monopole antenna is prearranged by Eq. (1).

$$f_r = \frac{144}{l_1 + d_1 + h + \frac{A_1}{2\pi\sqrt{\in_r+1}} + \frac{A_2}{2\pi\sqrt{\in_r+1}}} \tag{1}$$
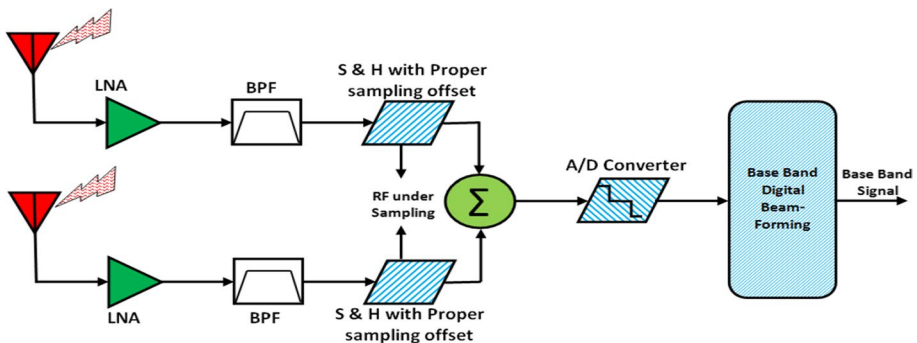

Fig. 1 A generic block diagram of two-element UWB–MIMO antenna-based receiver station
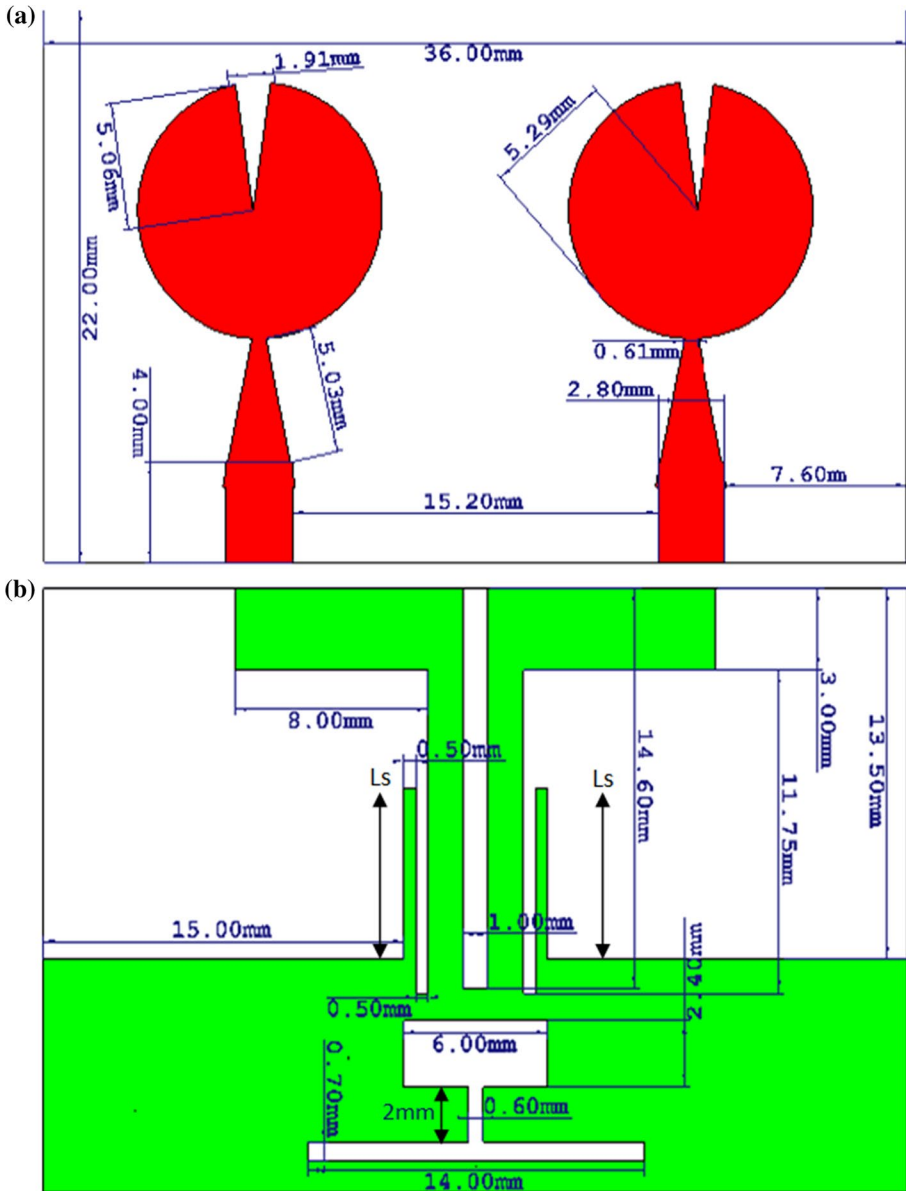
Fig. 2 Two-element UWB planar monopole MIMO antenna **a** front view, **b** bottom view

where A_1, A_2 is the area of anticipated radiation patches and ground plane, l_1, length of the ground plane, d_1, diameter of circular radiated patches. Step by step procedure of the proposed UWB-MIMO antenna design is ushered in Fig. 3 and corresponding return loss and isolation are presented in Fig. 4a and b respectively. Antenna-1 provides unsatisfactory return loss and isolation in intentional UWB range. By changing the feeding line width of antenna-1, return loss and isolation is improved as depicted in antenna-2.
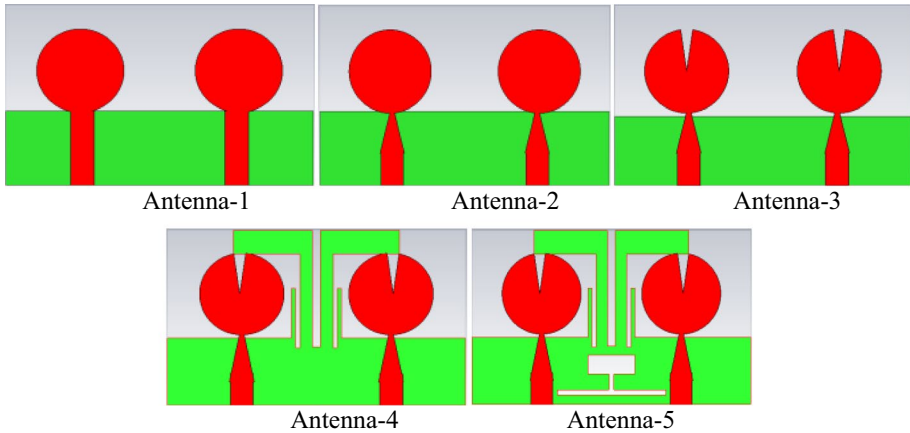
Fig. 3 Geometrical design steps of a designed antenna with WLAN band-notch characteristic
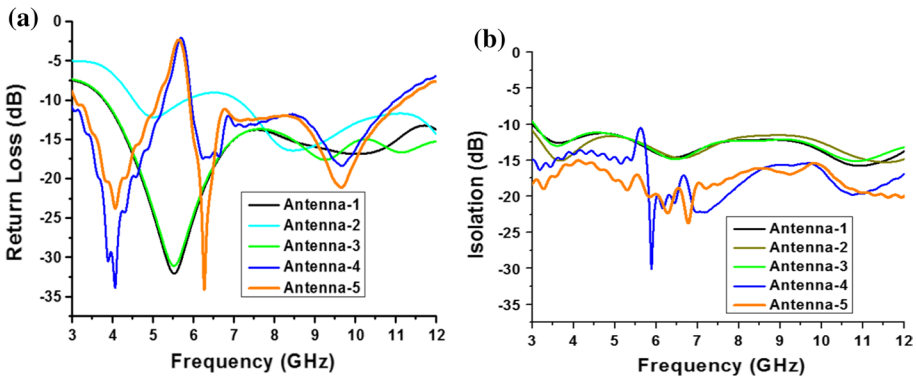

Fig. 4 Simulated (using CST MWS) results of **a** return loss, **b** isolation of the antennas shown in Fig. 3

In antenna-3, a triangular shape etched from patches which improve isolation as well as return loss. Hence, an antenna-4, impart vertical stubs on the ground plane to get better return loss from 3.1 to 4.8 GHz and it also provides a notch band characteristics for WLAN (5.1–5.9 GHz) although poor isolation in the intended lower frequency region. Therefore, to improve isolation in entire UWB bandwidth, fixed another T and I shaped slot in ground, the same as shown in antenna-5.

The notched band can be achieved by varying the ground stubs length (L_s) at the notch frequency, $f_n = c / \left(2 \times L_s \times \sqrt{\varepsilon_{reff}} \right)$, where c is the speed of the signal in a vacuum (3×10^8 m/s), ε_{reff} is the effective relative permittivity [23] of the substrate and approximated length of L_s is 6.3 mm at notched frequency.

Frequency selectivity of the rejection band is an important parameter to design a UWB antenna with notch band. For selectivity of the notched band of the UWB–MIMO antenna, another ubiquitous parameter is 'Roll off rate' i.e. control required a bandwidth of the WLAN band. Furthermore, RoC-Roll off criteria is the ratio of the bandwidth at −5 dB and −10 dB, i.e. RoC = $BW_{-5\ dB}/BW_{-10\ dB}$ and the RoC of proposed antenna is 0.44, which is acceptable for practical design. The bandwidth of notched
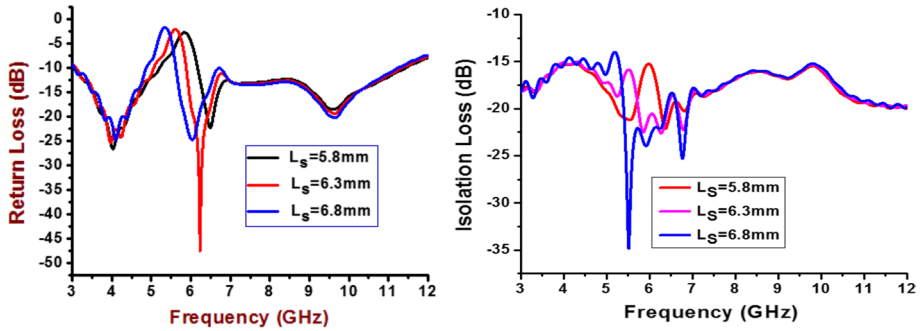
Fig. 5 Simulated results of return loss and Isolation of antenna with a variation of length of stubs (L_s) in the ground plane
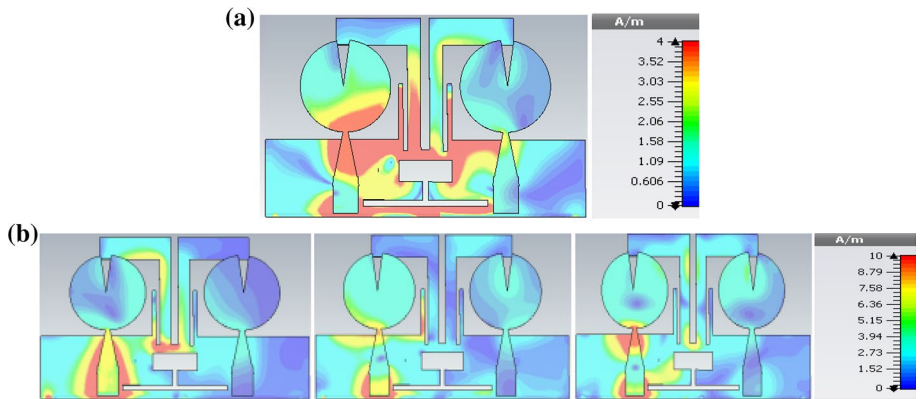
Fig. 6 Surface current distributions at **a** notch band frequency i.e. 5.6 GHz and **b** 4.1, 6.6 and 9.6 GHz when port-2 terminated with 50 Ω impedance and port-1 is excited

band is also controlled by the length of stubs (Ls) in ground plane and the results of return loss, centered at 5.6 GHz as made known in Fig. 5. By varying Ls from 5.8 to 6.8 mm, return loss curve shifts from higher to lower frequency and value of return loss at the intended notch (6.3 mm) is − 2.0 dB. Impedance bandwidth is also maintained significantly, in the entire bandwidth throughout optimization of L_s.

It is hardnosed from Fig. 6a, where strong current accumulates around vertical stubs in the ground plane, which produces a notched for WLAN band in UWB bandwidth to mitigate interference. Figure 6b shows the distribution of current on the antenna at various frequencies like 4.1, 6.6 and 9.6 GHz respectively. It is too observed that the flows of current on the tapered feed line to circular element while a small current pours across the second element of MIMO. The slot in ground plane works as an isolator between the two elements and this is preventing the coupling of the electromagnetic energy.

3 Results and Discussion

The scattering parameter results (measured and simulated) are shown in Fig. 7. Eventually, measured S_{12} shows better isolation than the simulation results and isolation between two antenna radiators is < -30 dB for the entire UWB bandwidth. Results illustrate that the return loss of proposed MIMO antenna is ≤ -10 dB except for notched band (WLAN) and bandwidth of the antenna is 8.1 GHz (from 3.1 to 11.2 GHz), that fulfills the FCC requirement for UWB applications without interference.

Maximum peak gain of antenna has revealed the better conformity between simulated and measured results and the maximum value of gain is 4.85 dB. The radiation efficiency of antenna throughout the requisite band is higher than the permissible limit except for the notched band, is centered at 5.6 GHz. Consequently, proposed MIMO can appropriate to work in the high interference surrounding as presented in Fig. 7b.

Figure 8a–c shows the 3D radiation pattern of proposed MIMO antenna at 4.1, 6.6 and 9.6 GHz frequency correspondingly, when port-1 is excited and port-2 is terminated with 50 Ω or vice versa. Radiation patterns are slightly directional because power radiated towards the left of the yz-plane when port-1 is excited and when port-2 of MIMO antenna is excited, the power is radiating towards the right of the yz-plane to achieved pattern diversity performance of an antenna. Co-polarization is the power level of an electromagnetic wave in an intended direction on the other hand cross-polarization is the power level of an electromagnetic wave in an un-intended direction due to interference at reception or transmission antenna. Co-polarization and Cross-polarization at different frequencies are calculated by the simulator (CST-Microwave studio) and validate these results by Vector Network Analyzer so we use two terms simulated, by CST-Microwave studio and measured by VNA. The prototype of proposed MIMO antenna on FR-4 substrate is fabricated by conventional printed circuit board design procedure and antenna under test in an anechoic chamber associated with VNA for measurement of radiation characteristics as shown in Fig. 8d and e.

Figure 9 shows the simulated/measured yz-plane (left) and xz-plane (right) radiation pattern of antenna at three different frequencies as 4.1, 6.5 and 9.6 GHz respectively with an acceptable agreement. Whereas the UWB–MIMO antenna consists of two indistinguishable radiated antenna elements and so the time of measurement of the 2D radiation pattern, port-1 is excited and port-2 is terminated by the 50 Ω load. It is observed that at operating
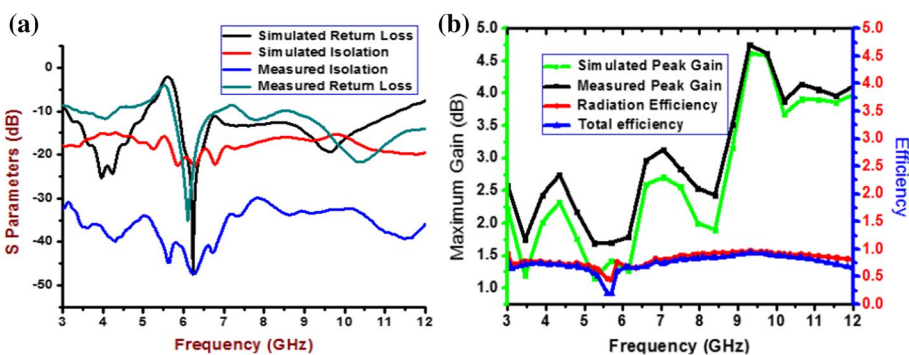
Fig. 7 Simulated and measured **a** S-parameter (Return and Isolation) **b** peak gain, radiation efficiency and total radiation efficiency of UWB–MIMO antenna
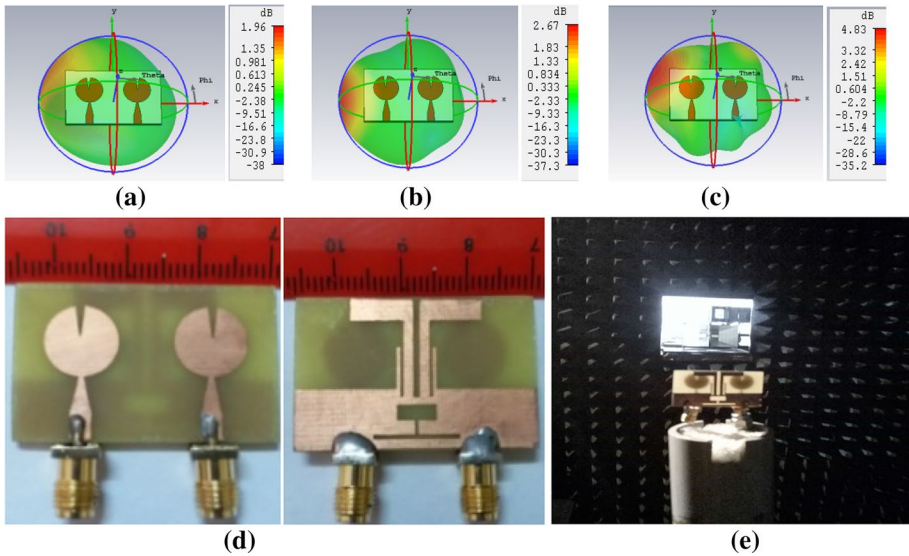
Fig. 8 The 3D radiation pattern of MIMO antenna at **a** 4.1 GHz, **b** 6.6 GHz, **c** 9.6 GHz only port-1 is excited and port-2 terminated by 50 Ω load, **d** fabricated prototype, **e** antenna under test in an anechoic chamber for radiation pattern measurement

frequency band the radiation patterns are omnidirectional in H (xz)-plane and dipole like in E (yz)-plane except for WLAN band. The splitting of the radiation lobes is also observed due to higher-order mode propagation at higher frequencies.

Specific absorption rate: SAR is a vital parameter in the antenna at which the human body is absorbed electromagnetic field energy when exposed, means the power absorbed per mass of body/head tissue as shown Fig. 10. It is typically averaged either over a small sample volume (typically 1 g or 10 g of tissue) or over the entire body. The SAR value of any RF and microwave electronic devices is obtained by penetration of electric field intensity in the human head tissue at near field environment [24, 25]. Furthermore, SAR estimation on the head at 4.1, 6.6 and 9.6 GHz frequency, the skin radius, bone radius, and brain radius are 79.324 mm, 75 mm and 65 mm respectively are used and other parameters are also listed in Table 1. The calculated value of SAR is less than 1.6 W/kg for the proposed antenna design as shown in Table 2 but this SAR performance investigates without any plastic jacket or cover, thus when we wrap proposed antenna into a plastic jacket or cover then SAR performance may be increased more. SAR for electromagnet energy is calculated by Eq. (2).

$$\text{SAR} = \frac{1}{V} \int \frac{\sigma(r)|E(r)|^2}{\rho(r)} dr \tag{2}$$

where σ = thermal conductivity of sample in S/m, E_{rms} = electric field in V/m, ρ = sample density in kg/m^3, V = volume of the sample in m^3.
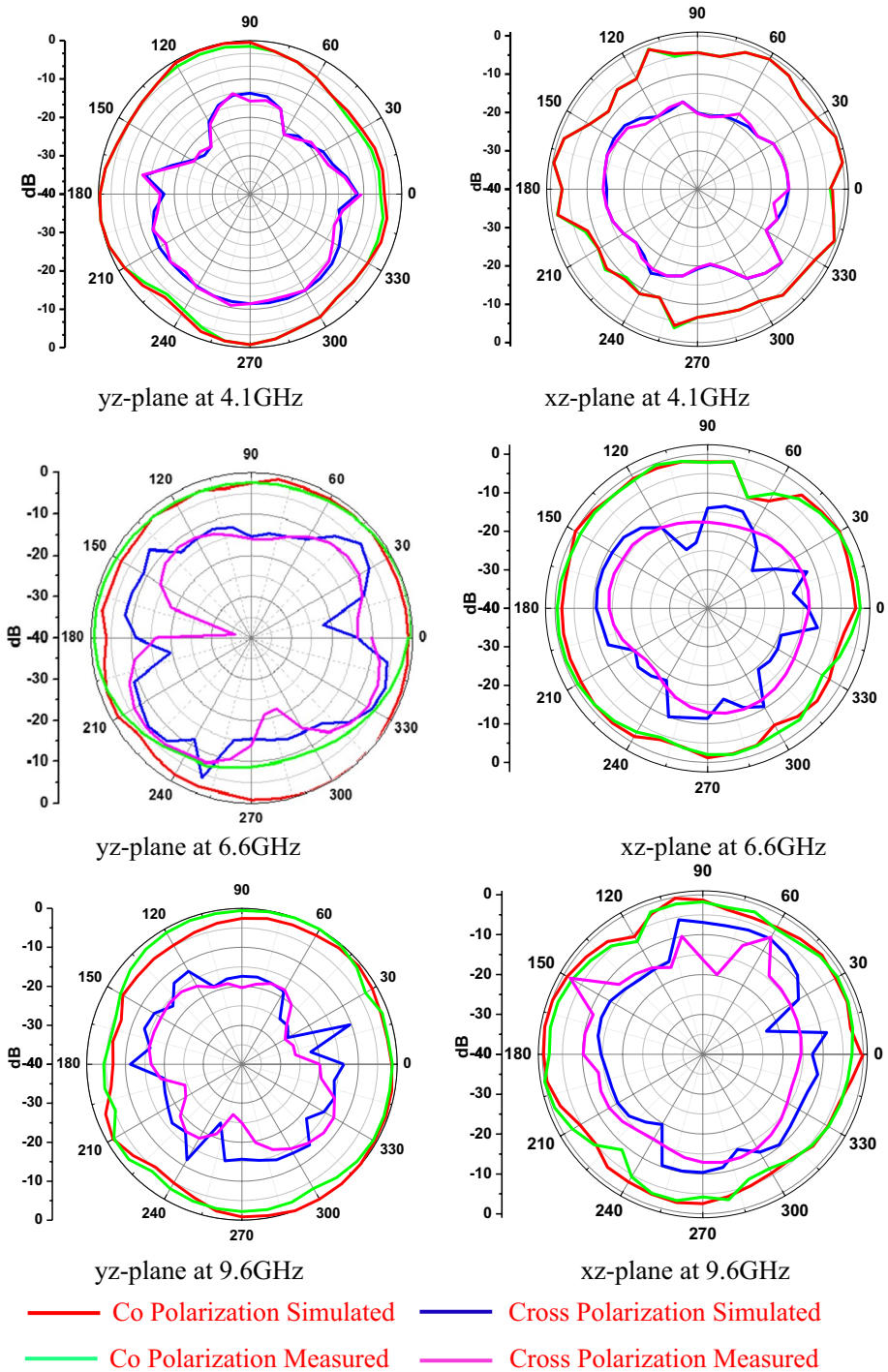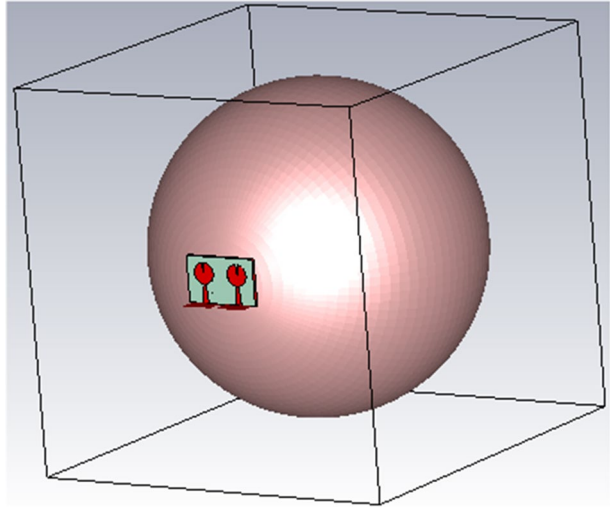
Fig. 9 Measured and simulated 2D radiation pattern at 4.1, 6.6 and 9.6 GHz for yz-plane (left) and xz-plane (right)

Fig. 10 Calculation of specific absorption rate near the human head in presence of the proposed MIMO antenna

Table 1 Parameters of the human head for calculation of specific absorption rate (SAR) by the proposed antenna at constant permeability (i.e. 1)

Type	Density (ρ) (kg/m^3)	Thermal conductivity (σ) (S/m)	Heat capacity (kJ/K/kg)	Blood flow (W/K/m^3)	Metabolism rate (W/m^3)
Bio-tissue skin	1100	0.293	3.5	9100	1620
Bio-tissue bone	1850	0.41	1.3	3400	610
Bio-tissue brain	1030	1.13	3.675	40,000	7100

Table 2 SAR values near the human head at different resonant frequencies when the distance between the human head and MIMO antenna is 13 mm

Specific absorption rate (W/kg)					
4.1 GHz		6.6 GHz		9.6 GHz	
1 (g)	10 (g)	1 (g)	10 (g)	1 (g)	10 (g)
1.28	0.86	1.39	0.93	1.49	1.04

4 MIMO Diversity Performance

MIMO diversity performance of the proposed antenna is evaluated in terms of Envelope Correlation Coefficient, Total Active Reflection Co-efficient, Diversity Gain, Multiplexing Efficiency and Channel Capacity Loss. The mutual coupling between two radiation patches and the amount of correlation between them is examined by ECC. It is calculated through using S-parameters by following Eq. (3a) and this equation is valid for measuring of ECC when the antenna is lossless and radiated power is uniformly distributed along with the antennas.

$$\text{ECC} = \frac{\left|S_{11}^* S_{12} + S_{21}^* S_{22}\right|^2}{\left(1 - |S_{11}|^2 - |S_{21}|^2\right) \times \left(1 - |S_{22}|^2 - |S_{12}|^2\right)} \tag{3a}$$

But lossless is a hypothetical result which varies from empirical result so, the computation the ECC of the MIMO antenna by Eq. (3b) in terms of radiated fields

$$\text{ECC} = \frac{\left|\iint\limits_{4\pi} \left[E_i(\theta, \phi) \times E_j(\theta, \phi)\right] d\Omega\right|^2}{\iint\limits_{4\pi} |E_i(\theta, \phi)|^2 d\Omega \times \iint\limits_{4\pi} |E_j(\theta, \phi)|^2 d\Omega} \tag{3b}$$

where E_i and E_j are the radiated electric fields vector of the ith and jth elements of the MIMO antenna system and Ω denotes beam area.

The ideal value of ECC is zero for uncorrelated MIMO antenna but their acceptable value for practical MIMO antenna is ≤ 0.5 and as per Fig. 11a the value of ECC of designed MIMO antenna is less than 0.01 in UWB bandwidth excluding notched band. Hence, the above result specifies pretty low correlation between the two antenna ports, which shows the excellent diversity performance. The diversity gain can be calculated by $\text{DG} = 10 \times \sqrt{\left(1 - \text{ECC}^2\right)}$ and for satisfactory operation of MIMO antenna diversity gain should be closed to 10 dB and the value of diversity gain of UWB-MIMO antenna is 9.95 dB apart from the notched band as depicted in Fig. 11a.

In addition, to optimize the antenna channel capacity, the multiplexing efficiency is a maneuver parameter which is not only explored the total antenna efficiency, but also the co-relation and efficiency disparity. In addition, multiplexing efficiency (η_{MUX}) is the ratio of the power requirement of an antenna to the reference antenna. Figure 11b shows the multiplexing efficiency of the MIMO antenna and η_{MUX} is calculated by $\eta_{\text{MUX}} = \sqrt{\left(1 - |\rho_c|^2\right) \eta_1 \eta_2}$, where ρ_c is a complex correlation between two side by side antenna i.e. $\text{ECC} = \rho_c^2$ and η_1, η_2 is the antenna total efficiency of MIMO antenna elements.
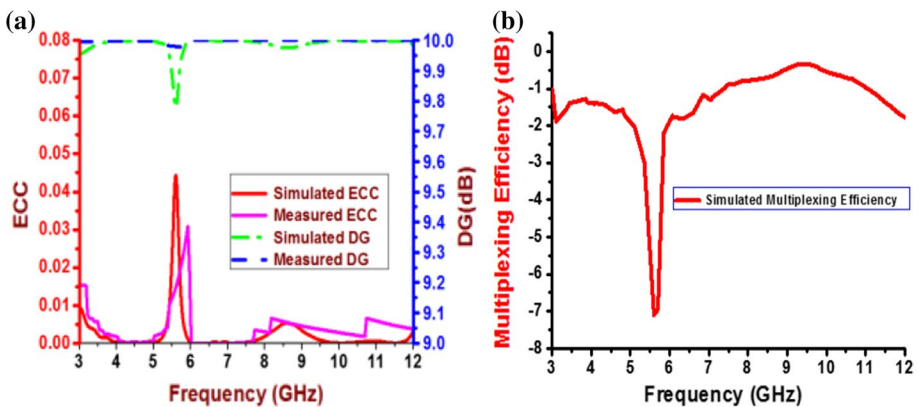

Fig. 11 Simulated and measured results of the proposed antenna **a** envelope correlation coefficient and diversity gain, **b** simulated result of multiplexing efficiency

The result shows that the total efficiency (shown in Fig. 7b) and multiplexing efficiency are almost identical and its value goes downward at notched WLAN band.

The two-port antenna system, contiguous antenna elements impinge on each other and when working concurrently they influence the overall desirable gain, efficiency, and bandwidth. Actual MIMO antenna system performance will not be predicted by S-parameters only, therefore TARC has initiated this effect into account. It is the square root of the ratio of total reflected to total incident power and hence, it gives the information about the apparent return loss of the MIMO antenna system. For side by side two port radiated antenna system, it can be evaluated by Eq. (4).

$$\text{TARC} = \sqrt{\frac{(S_{11} + S_{12})^2 + (S_{22} + S_{21})^2}{2}} \qquad (4)$$

Ideally, the value of TARC should be less than 0 dB for MIMO antenna based system. Figure 12a shows the simulated and measured TARC of the proposed MIMO antenna and it is observed that the value of TARC is less than -28 dB and -40 dB correspondingly in the entire UWB range except for the notched band, it shows the excellent diversity performance of the designed antenna. With increasing the number of elements, the channel capacity of MIMO system is linearly increased, so the element matrix properly characterizes the performance of a MIMO system as it provides the information about the phase and gain characteristics of the transmitting and receiving elements. However, in the presence of the correlation factor in MIMO antennas, the channel capacity losses are also increased. Therefore, diversity performance of proposed antenna pretentious and channel capacity losses are calculated by the following Eq. (5)

$$\text{CCL(dB)} = -\log_2\left[\det\left(\phi^R\right)\right] \qquad (5)$$

where ϕ^R is the 2×2 co-relation matrix in terms of S-parameter $\varphi_{ii} = 1 - |S_{ii}|^2 - |S_{ij}|^2$, $\varphi_{ij} = -(S_{ii} \times S_{ij} + S_{ji} \times S_{jj})$. Figure 12a shows the CCL losses and it is less than 0.35 bits/s/Hz over the entire bandwidth except for notch band, which offer a better diversity results of the proposed MIMO antenna. Moreover, the mean effective gain
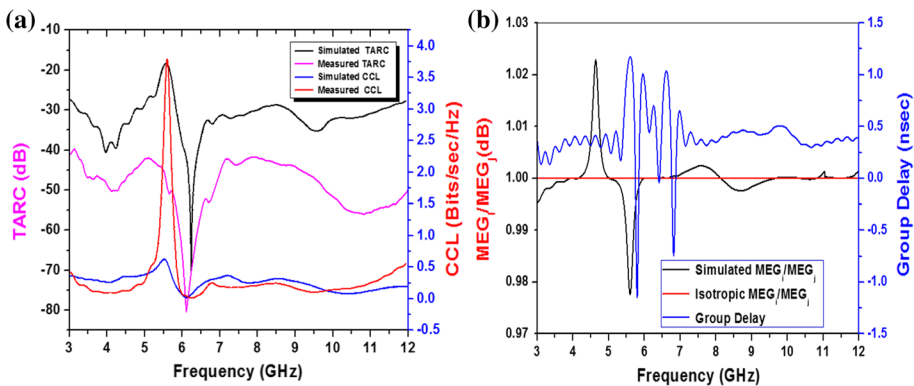
Fig. 12 Simulated and measured results of **a** channel capacity loss (CCL) and total active reflection coefficient (TARC), **b** simulated results of the mean effective gain (MEG) and group delay of proposed MIMO antenna

(MEG) is the ratio of the mean received power by the ith antenna to the mean incident power of the jth antenna with the same route, $MEG_i = \varepsilon_{Total}/2$, where ε_{Total} is implying total effective efficiency of the ith antenna, i.e. $\varepsilon_{Total}^i = \varepsilon_{mis}^i \times \varepsilon_{rad}^i$, and where $\varepsilon_{mis}^i = 1 - \sum_{j=1}^{N} |S_{ij}|^2$, $\varepsilon E_{rad}^i = \sum_{j=1}^{N} |S_{ij}|^2$ where ε_{mis}^i, and ε_{rad}^i are mismatch efficiency and radiation efficiency of ith antenna as shown in Fig. 12b. MEG ratio for the proposed MIMO antenna is to be extracted by Eq. (6)

$$MEG_i = \frac{P_{rec}}{P_{inc}} = \oint \left[\frac{XPR \times G_{\theta i}(\Omega) + G_{\phi i}(\Omega) \times P_{\phi}(\Omega)}{1 + XPR} \right] d\Omega \tag{6}$$

where, XPR is the cross-polarization ratio, $G_{\theta i}(\Omega)$, $G_{\phi i}(\Omega)$ and $P_{\phi}(\Omega)$ is the gain and power density function of the incident wave, $\Omega =$ beam area.

The acceptable ratio of mean effective gain of ith and jth antenna elements should be less than or equal to ± 3 dB and as from Fig. 12b, the MEG ratio of the projected MIMO antenna found in acceptable limit throughout the UWB range, which is a high-quality channel performance for wireless communication. Finally, to verify the time domain analysis of the intended MIMO antenna, two identical antennas have located in front of each other as a receiver and transmitter at a distance of 100 cm and group delay (ns) is calculated. Group delay is the rate of change of transmission phase angle with respect to frequency and it is almost constant in entire the intended band. Group delay in terms of return loss (S_{11}) is defined by equation $T_d(\omega) = -\delta\phi/\delta\omega$, where $\Phi =$ phase of S_{11} and $\omega =$ angular frequency in rad/s. The group delay deviation of proposed MIMO antenna is ≤ 0.3 ns entire the UWB frequency span excluding notched band as shown in Fig. 12b.

The MEG is also represented in isotropic and Gaussian mediums, to investigate the diversity performance at XPR $= 0$ dB (outdoor) and 6 dB (indoor) as shown in Fig. 13a and Table 3 of the proposed antenna. The MEG for the isotropic medium at 0 dB and 6 dB XPR is constant at -3.0 dB and lies between -3.1 and -5.1 dB respectively. Similarly, the MEG for Gaussian medium at 0 dB and 6 dB XPR is lying between -2.7 and -4.2 dB, and -4.6 to -6.5 dB respectively for entire UWB bandwidth.
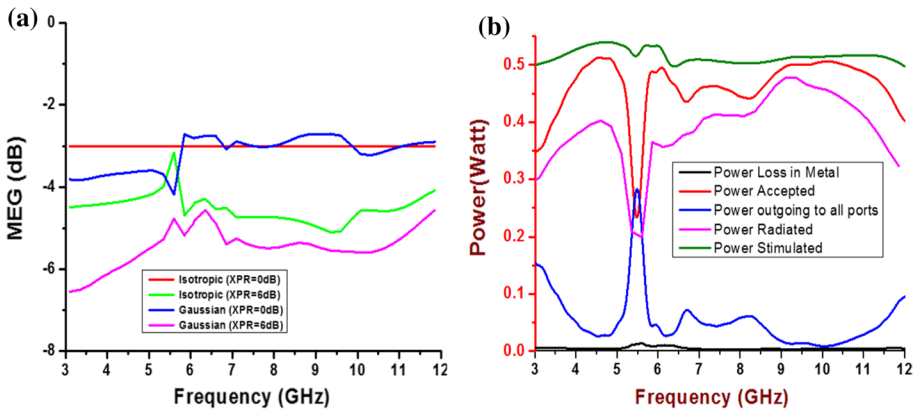
Fig. 13 **a** A simulated mean effective gain in Isotropic and Gaussian medium at various XPR values of proposed antenna applications, **b** power associated with proposed MIMO antenna for various diversity performances

Table 3 Simulated MEG results of proposed MIMO antenna at various frequencies

Frequency (GHz)	MEG (dB) Isotropic medium		MEG (dB) Gaussian medium	
	XPR = 0 dB	XPR = 6 dB	XPR = 0 dB	XPR = 6 dB
4.1	− 3.0	− 4.4	− 3.7	− 6.1
6.6	− 3.0	− 4.5	− 2.8	− 4.9
9.6	− 3.0	− 5.1	− 2.7	− 5.6

The power loss, power accepted, power outgoing, power radiated, and power stimulated of the proposed antenna is used to calculate the parameters like SAR, CCL, ECC, DG and radiation efficiency as shown in Fig. 13b. 0.5 W stimulated power is used to calculate all MIMO antenna parameters. Stimulated power, accepted power, and power radiated is having the same nature with different values due to various losses like a dielectric, conductor, surface wave, and port losses. Therefore, stimulating power is always greater than accepted and radiated power. Power going to all ports is highly interfere at the notched band (5.1–5.85 GHz) so that the maximum power is correlated between ports and not used for radiation.

An evaluation of the proposed MIMO antenna with existing referred MIMO antennas is represented in Table 4. It is observed that the designed antenna achieves the better results in comparison with the most of the MIMO antennas at various specifications, which is highly appreciable as small in size, low in cost, improved radiation efficiency (0.75–0.97) with enhanced isolation, better ECC and diversity gain (> 9.95 dB).

Table 4 Comparison of proposed UWB-MIMO antenna including WLAN notched band with existing references at various aspects

Antenna size (mm^2)	Isolation (dB)	Frequency (GHz)	ECC	DG (dB)	Material	Radiation efficiency
50×90 [2]	> 12	1.8–5.2	< 0.33	> 9.50	RO4350B	> 0.63
50×40 [3]	> 15	2.5–11	< 0.02	> 9.65	FR-4	> 0.692
50×82 [5]	> 15	2.15–13.62	< 0.04	> 9.79	FR-4	0.6-0.85
23×18 [6]	> 15	3–12.4	< 0.015	> 9.90	F4b2	> 0.70
36×18 [7]	> 20	2.8–20	< 0.03	> 9.95	FR-4	> 0.692
23×29.8 [3]	> 21	2.5–12	< 0.01	> 9.95	Rogers TMM4	0.55–0.82
40×40 [9]	> 15	2–6	< 0.1	> 9.95	FR-4	0.5–0.85
26×15 [11]	> 24	2–35	< 0.03	> 9.90	FR-4	> 0.50
55×13.5 [13]	> 18.3	1.92–10.6	< 0.019	> 9.95	FR-4	> 0.91
36×22 [Proposed]	> 30	3.1–11.2	< 0.008	> 9.95	FR-4	0.75–0.97

5 Conclusion

A MIMO antenna has been designed for UWB bandwidth (3.1–11.2 GHz) with better isolation (≤ -30 dB), radiation efficiency (> 0.75), and sharp rejection at WLAN (5.1–5.85 GHz) band. Diversity performance of antenna has also been verified in terms of ECC (≤ 0.008), TARC (≤ -25 dB), CCL (≤ 0.3 bits/s/Hz), Mean effective gain ratio (MEG$_i$) $\cong 1$ and Directive Gain (≥ 9.95 dB). Apart from the above-mentioned antenna performance, the SAR value of antenna, when it is used in human interface devices is less than the permissible limit as mentioned in Table 2, hence the antenna prototype is appropriate for UWB bandwidth at high interference surroundings in indoor or outdoor applications.

References

1. Li, Q., Feresidis, A. P., Mavridou, M., & Hall, P. S. (2015). Miniaturized double-layer EBG structures for broadband mutual coupling reduction between UWB monopoles. *IEEE Transactions on Antennas and Propagation, 63*(3), 1168–1171.
2. Dhar, S. K., Sharawi, M. S., Hammi, O., & Ghannouchi, F. M. (2016). An active integrated ultrawideband MIMO antenna. *IEEE Transactions on Antennas and Propagation, 64*(4), 1573–1578.
3. Lin, G.-S., Sung, C.-H., Chen, J.-L., Chen, L.-S., & Houng, M.-P. (2017). Isolation improvement in UWB MIMO antenna system using carbon black film. *IEEE Antennas and Wireless Propagation Letters, 16,* 222–225.
4. Mao, C.-X., & Chu, Q.-X. (2014). Compact radiator UWB-MIMO antenna with dual polarization. *IEEE Transactions on Antennas and Propagation, 62*(9), 4474–4480.
5. Toktas, A. (2016). G-shaped band-notched ultra-wideband MIMO antenna system for mobile terminals. *IET Microwaves, Antennas and Propagation, 11*(5), 718–725.
6. Tao, J., & Feng, Q. (2017). Compact ultrawideband MIMO antenna with half-slot structure. *IEEE Antennas and Wireless Propagation Letters, 16,* 792–795.
7. Chandel, R., Gautam, A. K., & Rambabu, K. (2018). Design and packaging of an eye-shaped multiple-input–multiple-output antenna with high isolation for wireless UWB applications. *IEEE Transactions on Components, Packaging, and Manufacturing Technology, 8*(4), 635–642.
8. Khan, M. S., Capobianco, A.-D., Naqvi, A., Ijaz, B., Asif, S., & Braaten, B. D. (2015). Planar, compact ultra-wideband polarisation diversity antenna array. *IET Microwaves, Antennas and Propagation, 9*(15), 1761–1768.
9. Sarkar, D., & Srivastava, K. V. (2017). A compact four-element MIMO/diversity antenna with enhanced bandwidth. *IEEE Antennas and Wireless Propagation Letters, 16,* 2469–2472.
10. Liu, L., Cheung, S. W., & Yuk, T. I. (2015). Compact MIMO antenna for portable UWB applications with band-notched characteristic. *IEEE Transactions on Antennas and Propagation, 63*(5), 1917–1924.
11. Gautam, A. K., Yadav, S., & Rambabu, K. (2018). Design of ultra-compact UWB antenna with band-notched characteristics for MIMO applications. *IET Microwaves, Antennas and Propagation, 12*(12), 1895–1900.
12. Lee, J.-M., Kim, K.-B., Ryu, H.-K., & Woo, J.-M. (2012). A compact ultrawideband MIMO antenna with WLAN band-rejected operation for mobile devices. *IEEE Antennas and Wireless Propagation Letters, 11,* 990–993.
13. Rajkumar, S., Selvan, K. T., & Rao, P. H. (2018). Compact 4 element S Sierpinski K nopp fractal UWB MIMO antenna with dual-band notch. *Microwave and Optical Technology Letters, 60*(4), 1023–1030.
14. Gao, P., He, S., Wei, X., Xu, Z., Wang, N., & Zheng, Y. (2014). Compact printed UWB diversity slot antenna with 5.5-GHz band-notched characteristics. *IEEE Antennas and Wireless Propagation Letters, 13,* 376–379.
15. Abedian, M., Rahim, S. K. A., Fumeaux, C., Danesh, S., Lo, Y. C., & Jamaluddin, M. H. (2017). Compact ultrawideband MIMO dielectric resonator antennas with WLAN band rejection. *IET Microwaves, Antennas and Propagation, 11*(11), 1524–1529.

16. Sengar, K., Rani, N., Singhal, A., Sharma, D., Verma, S., & Singh, T. (2014). Study and capacity evaluation of SISO, MISO, and MIMO RF wireless communication systems. ArXiv preprint arXiv :1403.7774.

17. Rajkumar, S., Sivaraman, N. V., Murali, S., & Selvan, K. T. (2017). Heptaband Swastik arm antenna for MIMO applications. *IET Microwaves, Antennas and Propagation, 11*(9), 1255–1261.

18. Liu, Guifeng., Liu, Ying., & Gong, Shuxi. (2017). Compact uniplanar UWB MIMO antenna with band-notched characteristic. *Microwave and Optical Technology Letters, 59*(9), 2207–2212.

19. Deng, J. Y., Wang, Z. J., Li, J. Y., & Guo, L. X. (2018). A dual-band MIMO antenna decoupled by a meandering line resonator for WLAN applications. *Microwave and Optical Technology Letters, 60*(3), 759–765.

20. Fang, H.-S., Wu, C.-Y., Sun, J.-S., & Huang, J.-T. (2017). Design of a compact MIMO antenna with pattern diversity for WLAN application. *Microwave and Optical Technology Letters, 59*(7), 1692–1697.

21. Ali, W. A., & Ibrahim, A. A. (2017). A compact double-sided MIMO antenna with improved isolation for UWB applications. *AEU-International Journal of Electronics and Communications, 82,* 7–13.

22. Ekrami, H., & Jam, S. (2018). A compact triple-band dual-element MIMO antenna with high port-to-port isolation for wireless applications. *AEU-International Journal of Electronics and Communications, 1*(96), 219–227.

23. Awasthi, Y. K., Singh, H., Sharma, M., Kumari, S., & Verma, A. K. (2017). Computer-aided design-based circuit model of microstrip line for terahertz interconnects technology. *The Journal of Engineering, 9*(7), 512–526.

24. Abd-Alhameed, R. A., Mangoud, M., Excell, P. S., & Khalil, K. (2005). Investigations of polarization purity and specific absorption rate for two dual-band antennas for satellite-mobile handsets. *IEEE Transactions on Antennas and Propagation, 53*(6), 2108–2110.

25. Iyama, T., Onishi, T., Tarusawa, Y., Uebayashi, S., & Nojima, T. (2008). Novel specific absorption rate (SAR) measurement method using a flat solid phantom. *IEEE Transactions on Electromagnetic Compatibility, 50*(1), 43–51.

Publisher's Note Springer Nature remains neutral with regard to jurisdictional claims in published maps and institutional affiliations.

Gaurav Saxena received his B. Tech degree in Electronics and Communication Engineering, from Uttar Pradesh Technical University Lucknow, India, in 2007, M. Tech degree in Microwave Electronics, from University of Delhi, South Campus, Delhi, India, in 2012. Currently, he is working an Assistant Professor in Galgotia College of Engineering and Technology, Greater Noida, Uttar Pradesh and Pursuing Ph.D. from Delhi Technological University, Delhi, India. His area of research interest are MIMO Antenna design for 5G wireless applications, Metamaterial absorber, and Microwave passive/active components.

Priyanka Jain received her B.E. degree in Electronics and Communication Engineering, M. Tech degree in Microwave Electronics, from the University Of Delhi, South Campus, Delhi, India, and Ph.D. from GGSIPU Delhi, India. Currently, she is working an Assistant Professor, Delhi Technological University, Delhi, India. She has published various articles in peer-reviewed journals and conferences. Her recent research interest includes Modeling of passive microwave components, Microwave antenna for 5G applications, Meta-material absorber, MIMO receiver/transmitter system, etc.

Yogendra Kumar Awasthi (M'13) received the B.Sc (Electronics) degree from Agra University, Agra, India in 1999, the M.Sc (Electronics and Computational Physics) degree from Agra University, Agra, India in 2001, in Electronics and Computational Physics and Ph.D. (RF and Microwave Engineering) from Delhi University, Delhi, in 2012. He was co-operative faculty in University of Delhi, New Delhi and he was also visiting faculty at Central Electronics Engineering Research Institute, Pilani, and Rajasthan, India in 2006–2012. He is currently working as Associate Professor with the Department of Electronics and Communication Engineering, Manav Rachna International Institute of Research and Studies, Faridabad, India. He has published more than 70 articles in peer-reviewed journals and conferences and he has also filed four patents and published one book's chapter. His recent research interest includes Modeling of high-frequency passive microwave components, Microwave antenna for LTE and 5G applications, Meta-material absorber, Sensor & Cloaking, Study of transient, RF Power Transfer and Energy Harvesting, MIMO receiver system, Electrical Power System, etc.